ORIGINAL ARTICLE

Effects of head size and morphology on dynamic responses to impact loading

Fang Wang · Heow Pueh Lee · Chun Lu

Abstract Head responses subjected to impact loading are studied using the finite element method. The dynamic responses of the stress, strain, strain energy density and the intracranial pressure govern the intracranial tissues and skull material failures, and therefore, the traumatic injuries. The objectivity and consistency of the prevailing head traumatic injury criteria, i.e., the energy absorption, the gravity centre acceleration and the head injury criterion (HIC), are examined with regard to the head dynamic responses. In particular, the structural intensity (STI) (the vector representation of energy flow rate) is calculated and discussed. From the simulations, the STI, instead of the gravity centre acceleration, the HIC and the energy absorption criteria, is found to be consistent with the dynamic response quantities. The different local skull curvatures at impact have a marginal effect whereas the locations of the impact loadings have significant effects on the dynamics responses or the head injury. The STI also shows the failure patterns.

Keywords Head dynamic responses · Head morphology · Head size · Finite element method · Structural intensity · Head injury criterion

F. Wang (✉) · H. P. Lee · C. Lu
Institute of High Performance Computing, 1 Science Park Road, #01-01 The Capricorn, Singapore Science Park II, Singapore, Singapore 117528
e-mail: wangf@ihpc.a-star.edu.sg
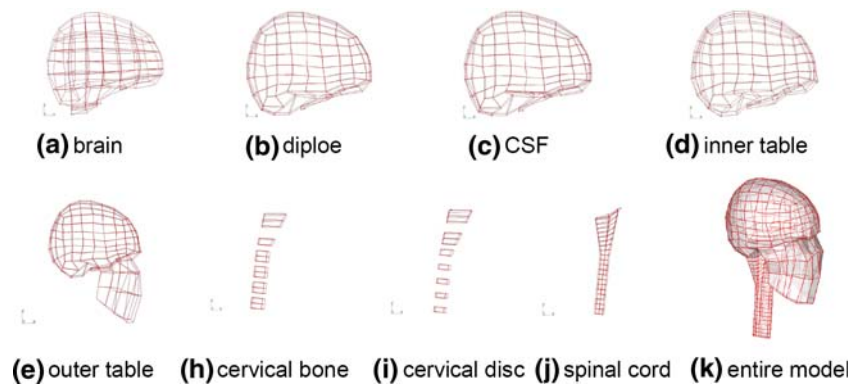
C. Lu
e-mail: luchun@ihpc.a-star.edu.sg

H. P. Lee
Department of Mechanical Engineering, National University of Singapore, 9 Engineering Drive 1, Singapore, Singapore 117576
e-mail: hplee@ihpc.a-star.edu.sg

1 Introduction

Head injury by road and domestic accidents causes substantial morbidity and mortality throughout the world, especially in developed countries. Much research effort from the biomechanics and neurotraumatic societies has been devoted to reveal head injury mechanics and the correlations with impact kinetics or kinematical inputs. In the head traumatic studies, early milestones can be attributed to Nahum and Smith's experimental model [1]. They measured the intracranial pressure and other dynamic response quantities under specific load intensities. Their work has been and is still being used to verify numerical models. Significant contributions also came from Ruan et al. [2], O'Donoghue and Gilchrist [3], Willinger et al. [4], Yoganadan et al. [5] and Zhang et al. [6]. Not only did they provide the in-vitro and in-vivo experimental data, they also built up very sophisticated finite element models for general head impact studies, as well as investigated the injury criteria for different types of traumatic injuries.

Head traumatic injuries have been identified, e.g. as concussion, axonal injury, hematoma, cerebrum contusion, skull fracture, etc. [6]. Different quantities are used for the evaluation of different types of injury, e.g., energy absorption criterion for skull fracture, coup/counter-coup pressures for intracranial contusions. Doorly et al. [7] suggested that the angular acceleration together with the strain rate be used for the prediction of subdural haematoma. An energy criterion and another tensile-strain-based criterion for skull fracture were introduced by Yoganadan et al. [5] and Vander et al. [8], respectively. Zong et al. [9] suggested another criterion of structural intensity (STI), which is a directional representation of the energy flow rate in a unit area. The STI is a compound index to integrate the dynamic response quantity of stress and the kinematical

Fig. 1 Head finite element model (Zong et al. [9])

(a) brain   (b) diploe   (c) CSF   (d) inner table

(e) outer table   (h) cervical bone   (i) cervical disc   (j) spinal cord   (k) entire model

quantity of velocity to reflect the injury locations and patterns.

However, assessment of head injury is far from straight forward because the pathological behavior of the injured could vary from person to person. The complete understanding of head trauma injury is further hindered by the paucity of in-vivo experimental data. On the other hand, numerical simulations contribute a great deal to the deep understanding of the phenomenon with its unique flexibility. The numerical models with verified mechanical fidelity allow the numerical simulation to reveal in detail head dynamic response scenarios under different impact loadings. Besides the aforementioned contributions [2–6, 9], it is worth mentioning that the first finite element head model was due to Hosey and Liu [10].

The present paper demonstrates through finite element simulations that under similar loading conditions, heads with similar sizes receive similar amounts of energy for the frontal and the side impacts. However, the head distributes the energy differently because of the different local structural configurations at the point of load impact. Local curvature changes at the forehead and temple have a marginal effect on the energy flow rate and other dynamic response quantities, whereas different locations of the load and head size are found to have significant effects. The STI rather than the energy absorption, gravity centre acceleration and HIC, may reflect these phenomena effectively. These findings conform to the general concepts regarding the head injury, i.e., 'the risk of injury is related to the energy delivered to the body by the impacting object as well as the object's shape' and 'the rate of loading and thus the strain rate is also an important factor in causing injury since biological tissues are viscoelastic [11–14].

2 Materials and methods

The FE model for the human head adopted in the present study, as shown in Fig. 1, contains five layers with variable thicknesses to approximate the basic average size adult human head structure [9]. The neck is composed of a spinal cord, a cervical bone and a disc. The mechanical fidelity of the model has been verified against Nahum and Smith's [1] and Trosseille et al.'s [15] impact tests. The geometrical data of this model are taken from Koenig [16]. A detailed description of this FE head model and its verification against experimental data are presented in Zong et al. [9]. Material properties of Young's modulus and Poisson's ratio for each material as listed in Table 1 are obtained from [17].

2.1 Elastic morphing method

Head size and shape vary from person to person and the same person at different ages. To evaluate the effect of different morphologies of the head while eliminating the effect of different head sizes, the finite element head model is modified with an elastic morphing method. The local curvatures of the frontal and temporal bones are changed by application of displacement boundary conditions at the local areas through a static elastic simulation. As shown in Fig. 2, nine nodes are moved normal to their respective initial local curvatures respectively. For convenience of notation, a unit curvature change is defined as a 4.5 mm outward displacement of the central point, while the surrounding eight nodes are separated by 3 mm displace-

Table 1 Material properties

Materials	Young's modulus (MPa)	Mass density (kg/m³)	Poisson's ratio
Outer table	5,465	3,000	0.22
Dipole	2,684	1,750	0.22
Inner table	5,465	3,000	0.22
CSF	0.1485	1,040	0.499
Spinal cord	0.1485	1,040	0.499
Cervical bone	5,465	3,000	0.22
Disc	7.5845	1,140	0.35
Brain	2.190	1,040	0.4996
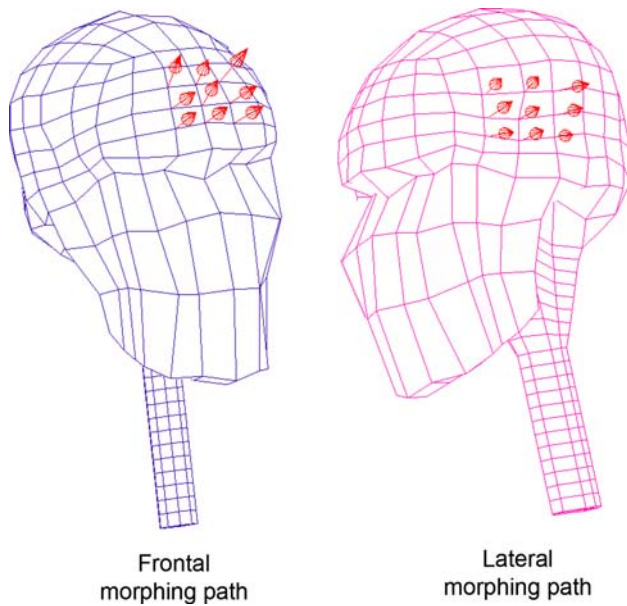
Fig. 2 Head frontal and side morphing paths

only to guarantee a convex forehead and concave temple. As a result, the forehead is extended by a maximum of 9 mm, while the temple is compressed by a maximum of 9 mm inward. Figure 3 illustrates the morphed curvatures for the frontal and side bones. The different curvature change levels are indicated by the unit numbers, e.g., m1 represents a minus unit change and 0 implies no curvature change. The morphed local curvatures for the frontal and side bones are quantitatively compared with evenly distributed radii over the areas (see Fig. 3). For the frontal bone, the average local radii are respectively, 122.86, 86.95, 70.03, 59.75 mm for the morphology states of m1, 0, 1 and 2, and –292.20 mm, –217.08, –143.61 mm, –110.29 mm for the concave side morphology states of m2, m1, 0, 1.

It should be mentioned that the magnitude of the morphing displacement came from the authors' understanding of the anatomical features of the human head. The authors felt the convexity of the frontal bone and concavity of the temple by touching with hand about a hundred office colleagues, who are from different regions and origins. However, the morphing unit displacement of maximum 4.5 mm is still highly hypothetic to study the different morphology effect indicatively.

The material properties for the head morphing simulation adopt the original values for the head tissues as listed in Table 1. The change of thickness of the skull is minimal since the Young's modulus of the skull is much higher than
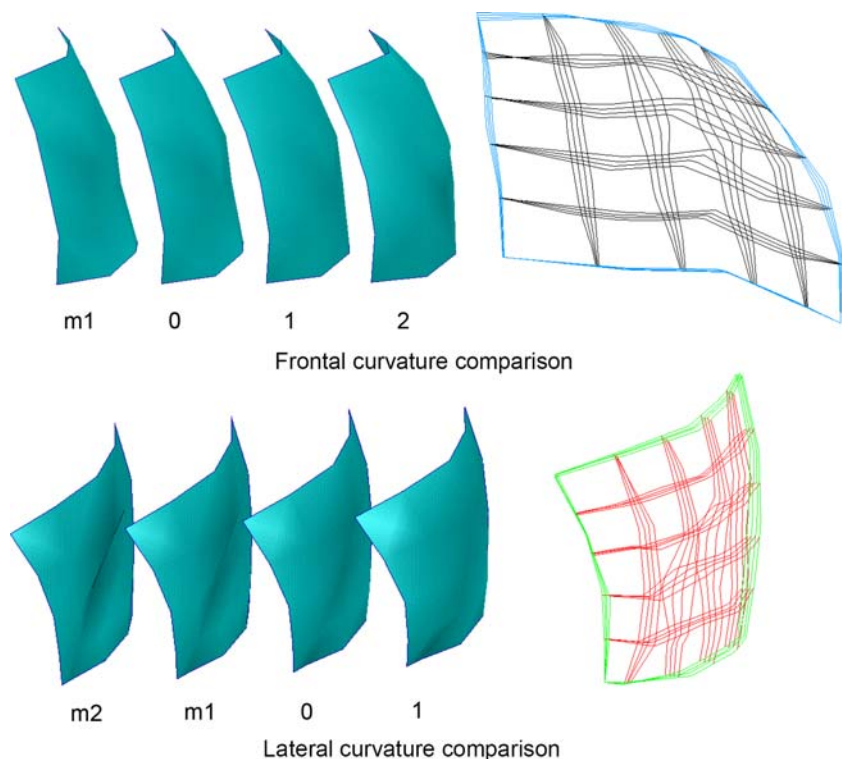
ments. Another nine nodes on the opposite side of the head are fixed. It should be mentioned that for the frontal curvature morphing simulation, the side curvature is kept unchanged and vise versa. For the forehead, the local curvature is increased by one and two units and reduced by one unit respectively, while for the temple, the curvature is reduced by one and two units and increased by one unit

Fig. 3 Morphed frontal and side curvatures

Frontal curvature comparison

Lateral curvature comparison
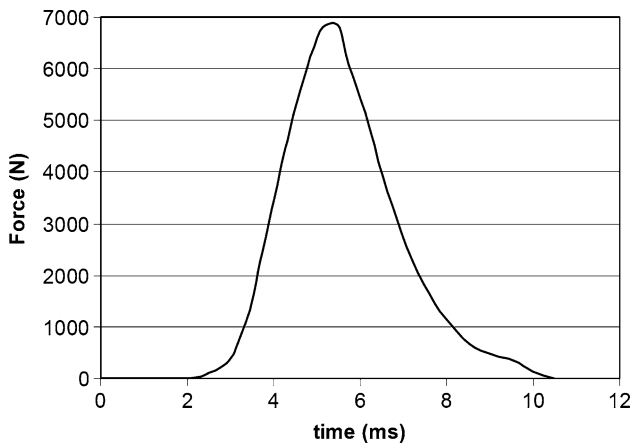
Fig. 4 Nahum and Smith's [1] force–time profile

Fig. 6 Comparison of force–displacement curves for frontal and side impacts

that of the soft intracranial tissues. Review of the morphed head models reveals that the change of the overall masses and the thicknesses of the skull are very minimal compared with the original head model. Deformed meshes are used for the following impact study.

2.2 Structural intensity

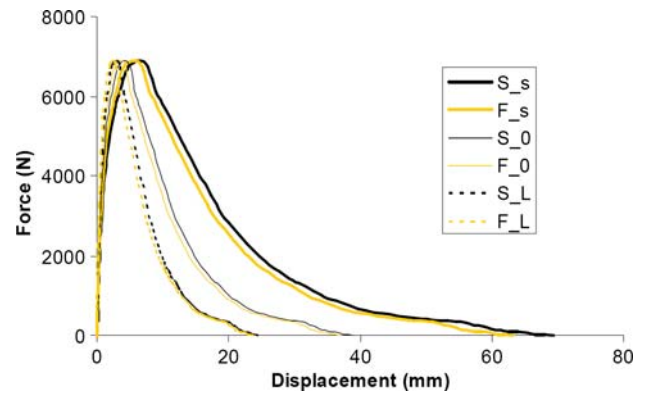The concept of STI, when it was firstly introduced by Noiseux [18], is defined as the power per unit width of

cross sectional area. It conforms to the concept of energy flux [18]. The STI is obtained at a set of points as a vector quantity, indicating the power flow direction and magnitude.

The mathematical form of the instantaneous components of STI in the time domain is

$$\text{STI}_i = -\sigma_{ij}(t)v_j(t), \tag{1}$$

where $\sigma_{ij}(t)$ is the component of the stress tensor and $v_j(t)$ is the velocity vector at time point t [19].
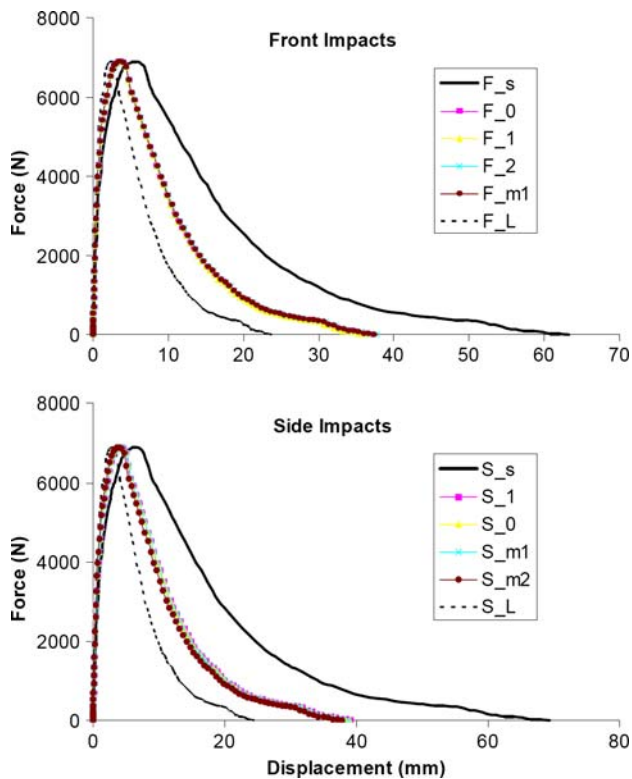

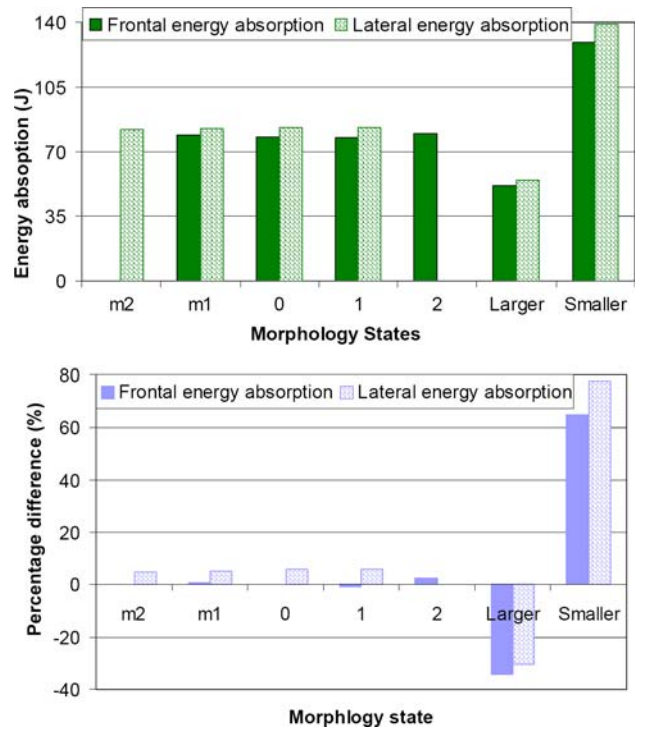Fig. 5 Force–displacement curves for frontal and side impacts

Fig. 7 Comparison of energy absorption for frontal and side impacts

Table 2 Energy absorptions

Morphology state	Frontal impact (J)		Side impact (J)	
	Absolute value	Difference (%)**	Absolute values	Difference (%)**
m2	NA*	NA*	82.1	4.942
m1	78.9	0.946	82.4	5.329
0	78.2	0.000	82.7	5.806
1	77.5	−0.864	82.9	5.982
2	80.1	2.468	NA*	NA*
15% larger	51.6	−34.00	54.4	−30.40
15% smaller	129.0	65.03	139.0	77.56

Note: NA* the data is not available; (%)** percentage difference with respect to the value from frontal impact on the original head model (morphology state of 0)

Table 3 Maximum first principal strains

Morphology state	Skull first principal strain				Brain first principal strain			
	Frontal impact		Side impact		Frontal impact		Side impact	
	Absolute value	Difference (%)**	Absolute values	Difference (%)**	Absolute values	Difference (%)**	Absolute value	Difference (%)**
M2	NA*	NA*	0.00336	118.31	NA*	NA*	0.192	14.11
M1	0.00145	−5.844	0.00324	110.45	0.178	6.071	0.195	16.13
0	0.00154	0.000	0.00301	95.71	0.168	0.000	0.203	20.71
1	0.00174	13.12	0.0028	82.01	0.160	−5.000	0.203	20.60
2	0.00151	−2.143	NA*	NA*	0.184	9.345	NA*	NA*
15% larger	0.00112	−27.01	0.0014	−9.091	0.117	−30.65	0.133	−20.77
15% smaller	0.00219	42.08	0.00447	190.39	0.231	37.62	0.277	64.76

Table 4 Maximum von Mises stresses

Morphology state	Skull von Mises stress (MPa)				Brain von Mises stress (MPa)			
	Frontal impact		Side impact		Frontal impact		Side impact	
	Absolute value	Difference (%)**	Absolute values	Difference (%)**	Absolute values	Difference (%)**	Absolute value	Difference (%)**
m2	NA*	NA*	30.49	17.90	NA*	NA*	0.130	19.63
m1	25.89	0.116	31.34	21.19	0.115	5.321	0.136	24.59
0	25.86	0.000	31.63	22.31	0.109	0.000	0.141	28.99
1	25.43	−1.663	30.68	18.64	0.105	−3.761	0.139	27.89
2	26.09	0.889	NA*	NA*	0.118	7.982	NA*	NA*
15% larger	19.13	−26.02	23.36	−9.667	0.076	−30.09	0.090	−17.77
15% smaller	37.18	43.77	45.55	76.141	0.151	38.44	0.193	76.70

3 Impact simulation results and discussions

Twelve cases are simulated with eight frontal and side impacts on the original head size with different local curvatures. Another four simulations on the 15% proportionally shrunk and enlarged head models are also implemented. The force—time profile from Nahum and Smith [1] as shown in Fig. 4 is applied on the same nine nodes for

Table 5 Maximum STI

Morphology state	Skull STI (J/m² s)				Brain STI (J/m² s)			
	Frontal impact		Side impact		Frontal impact		Side impact	
	Absolute value	Difference (%)**	Absolute values	Difference (%)**	Absolute values	Difference (%)**	Absolute value	Difference (%)**
m2	NA*	NA*	2.09E+08	27.44	NA*	NA*	1.42E+06	19.24
m1	1.57E+08	–4.024	2.14E+08	30.49	1.21E+06	1.765	1.50E+06	26.39
0	1.64E+08	0.000	2.13E+08	29.88	1.19E+06	0.000	1.55E+06	30.50
1	1.67E+08	1.524	2.04E+08	24.39	1.17E+06	–1.597	1.59E+06	33.28
2	1.55E+08	–5.470	NA*	NA*	1.22E+06	2.773	NA*	NA*
15% larger	7.97E+07	–51.38	9.94E+07	–39.37	5.50E+05	–53.82	8.95E+05	–24.83
15% smaller	3.90E+08	137.56	5.17E+08	214.94	2.59E+06	117.98	4.29E+06	260.13

Table 6 Maximum strain energy density

Morphology state	Skull strain energy density (J/mm³)				Brain strain energy density (J/mm³)			
	Frontal impact		Side impact		Frontal impact		Side impact	
	Absolute value	Difference (%)**	Absolute values	Difference (%)**	Absolute values	Difference (%)**	Absolute value	Difference (%)**
m2	NA*	NA*	1.05E+05	51.29	NA*	NA*	1.50E+04	41.89
m1	6.79E+04	–2.443	1.08E+05	54.89	1.11E+04	4.811	1.62E+04	52.36
0	6.96E+04	0.000	1.06E+05	52.16	1.06E+04	0.000	1.73E+04	63.40
1	6.98E+04	0.287	9.82E+04	41.09	9.78E+03	–7.773	1.70E+04	60.47
2	6.83E+04	–1.868	NA*	NA*	1.24E+04	16.981	NA*	NA*
15% larger	3.81E+04	–45.20	5.78E+04	–16.95	5.17E+03	–51.274	7.12E+03	–32.80
15% smaller	1.43E+05	105.89	2.19E+05	214.80	2.03E+04	91.792	3.27E+04	208.68

Table 7 Maximum brain pressure

Morphology state	Coup pressure (MPa)				Contra coup pressure (MPa)			
	Frontal impact		Side impact		Frontal impact		Side impact	
	Absolute value	Difference (%)**	Absolute values	Difference (%)**	Absolute values	Difference (%)**	Absolute value	Difference (%)**
m2	NA*	NA*	0.157	19.28	NA*	NA*	–0.155	10.48
m1	0.130	–0.610	0.168	28.28	–0.149	6.201	–0.157	11.62
0	0.131	0.000	0.188	43.37	–0.140	0.000	–0.115	–17.75
1	0.132	0.229	0.184	39.94	–0.133	–5.132	–0.162	15.75
2	0.130	–0.991	NA*	NA*	–0.153	9.195	NA*	NA*
15% larger	0.093	–29.19	0.125	–5.107	–0.104	–26.16	–0.117	–16.54
15% smaller	0.170	29.27	0.363	176.91	–0.210	49.96	–0.287	104.42

morphing displacements as seen in Fig. 2 for all impact simulations. The lower end of the neck could be set free or fixed according to Willinger et al. [4] since the loading time duration in the present study is very short (about 8 ms in Fig. 2). Thus the lower end of the neck is simply set free

in the present study. The ABAQUS explicit solver is used to solve the dynamic problem.

The calculated head force–displacement profiles under frontal and side impacts are plotted in Fig. 5. Different curvatures for the frontal and side impacts are found to
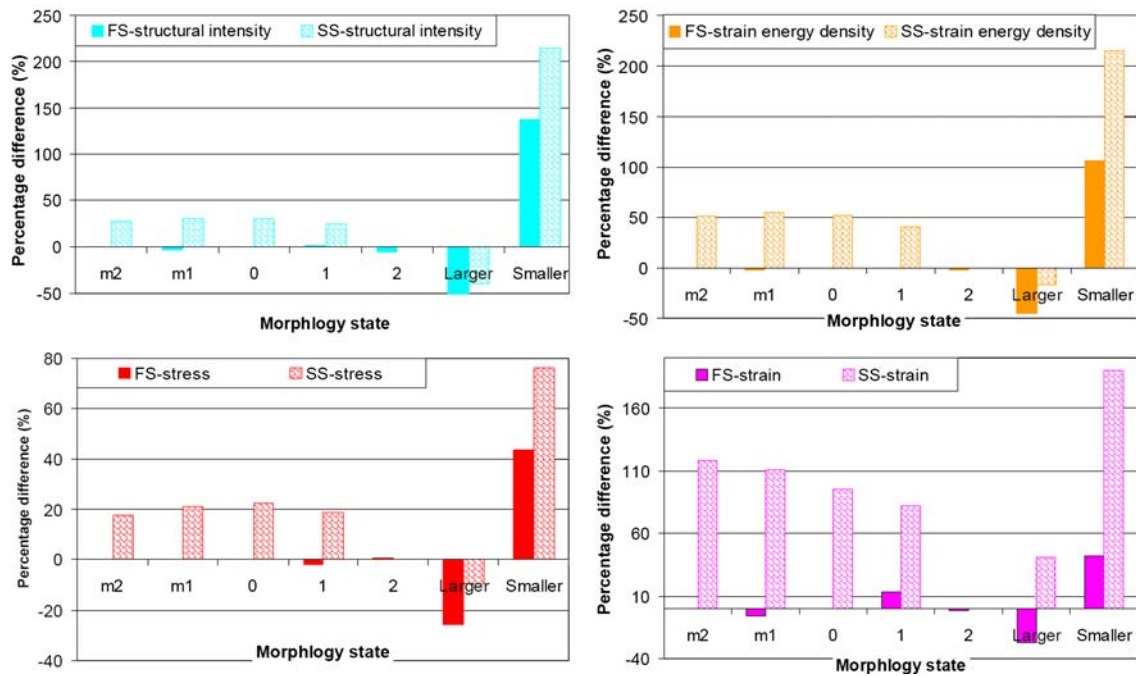
Fig. 8 Percentage differences of skull response quantities with respect to values from frontal impact on original head model

have minimal effect on the head kinematical response as seen in Fig. 5. Hence Fig. 6 compares only the force–displacement curves of the original reduced and the enlarged head models for frontal and side impacts. Figure 7 shows the energy absorptions by the head, which is the integral of the force–displacement curves of Fig. 5. Table 2 lists the energy absorptions and the percentage differences with regard to the data from frontal impact on the original head model. It is seen from Figs. 5, 6, 7 and Table 2 that energy absorption for either the frontal or side impacts of similar sized heads, are very similar. It is understandable that the force duration, magnitude and the head inertias yield similar energy absorptions. The different locations of the impact loading result in very slight differences, while the different head sizes have very significant influences. The smaller or larger head sizes have reduced or increased inertias respectively, which lead to remarkably different energy absorptions. The notation in Figs. 5, 6, 7 and all remaining figures is as follows: FS, SS denote skull quantities in frontal impact and side impact respectively, FB and SB indicate brain quantities, the following numerals indicate the curvature change units, while the letter of L or S represents the 15% larger or smaller head, respectively. It should be mentioned that all the percentage differences are calculated with respect to the values from the frontal impact on the original head model.

The head dynamic response quantities, i.e., the skull and brain stresses, strain, strain energy densities, intracranial pressures and the kinematical response quantities of gravity centre accelerations and HIC, are then examined and compared. The STI is also calculated according to Eq. 1.

Tables 3–7 list the maximum values of the dynamic response quantities, and the STI and their percentage differences with respect to the values from the frontal impact on the original head model. The histogram plots in Figs. 8 and 9 graphically illustrate the respective percentage differences for skull and brain dynamic response quantities and the STI. It is seen from Figs. 8 and 9 and Tables 4, 5, 6, 7 that the relative differences among the dynamics response quantities and the STI are quite consistent for both the skull and the brain. A clear tendency is found that the different curvature of the forehead or the temple has a marginal effect, the different locations of the impact loading result in remarkable differences, and the different head sizes have an even more prominent influence.

In contrast to the histogram plots for energy absorption in Fig. 7, the solid and shaded histograms denoting the frontal and side impacts respectively have striking differences in the plots for the dynamic response quantities in Figs. 8 and 9. Moreover, the local different curvature may also cause significant differences for the brain response quantities, especially for the strain energy density.

Figure 10 shows the respective gravity centre acceleration-time profiles for all the simulation cases. The representative frontal and side impact results are compared in Fig. 11. The HIC with 15 ms time intervals calculated
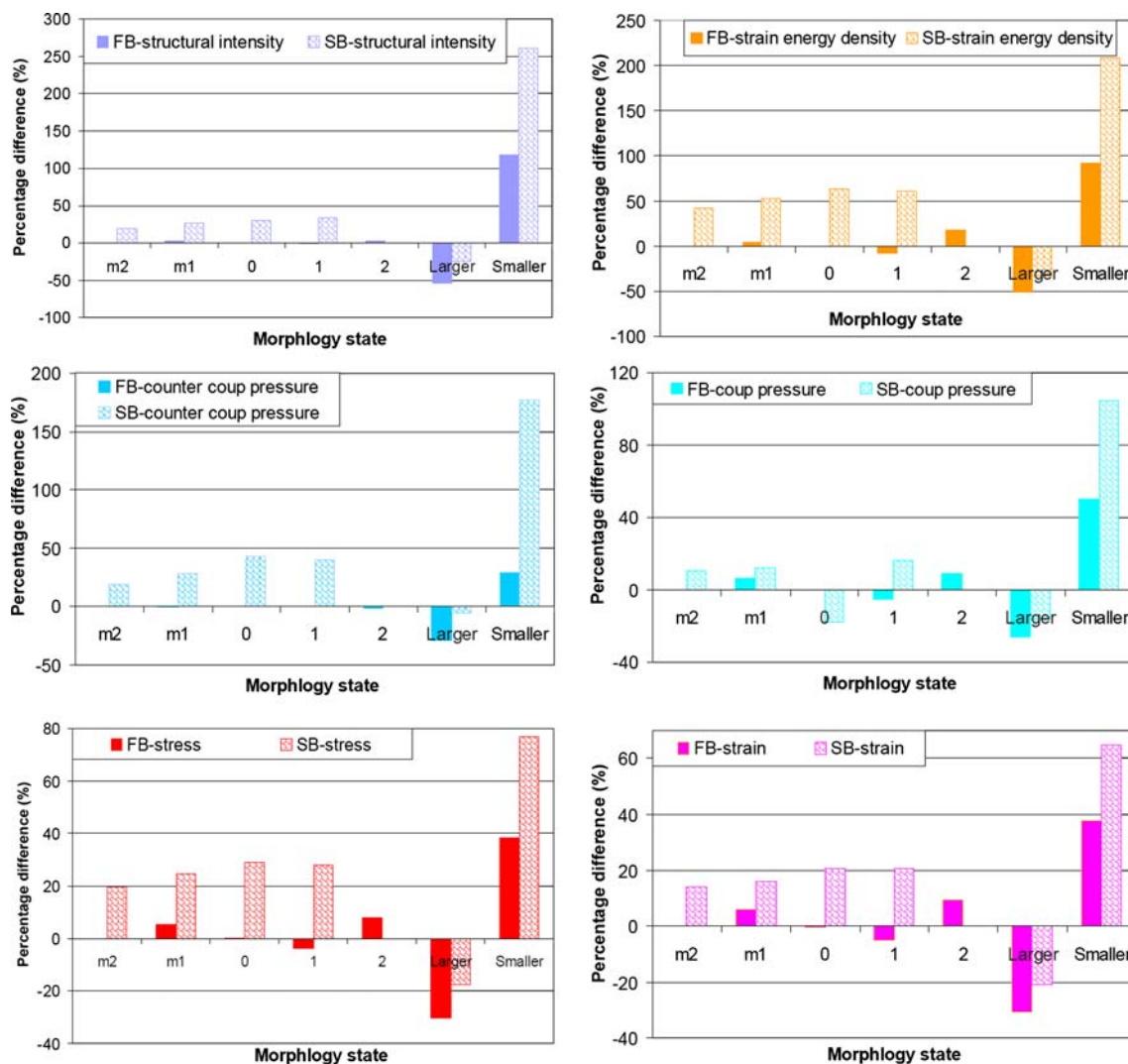
Fig. 9 Percentage difference of brain dynamic response quantities with respect to values from frontal impact on original head model

from Fig. 10, together with the gravity centre peak accelerations and their percentage differences, are tabulated in Table 8. Figure 11 illustrates the percentage differences. It should be mentioned that since the impact time duration is shorter than the 15 ms typical time interval for the HIC calculation, zero values are assumed for all time durations for which the acceleration is not available.

The kinematic quantities of gravity centre acceleration and HIC do not conform to the dynamics response quantities. It can be seen from the simulations as shown in Table 8 and Figs. 10 and 11 for the gravity centre acceleration and HIC that the different morphology state or curvatures of the forehead or the temple have a very minimal effect. The different loading locations and head size have very significant effects. The peak accelerations from the side impact increases by about half that of the counterparts involving frontal impact for a similar head

size, while the HIC from side impacts is almost four times as high as that from frontal impact.

4 Possible head injury locations and patterns

The distributions of the STI at the occasion that the highest value is found are shown in Fig. 12 for the brain and in Fig. 13 for the skull. For the brain in a side impact, both the distributions on the loaded and opposite sides are given for a clear presentation of the energy flow path. It can be observed that in the side impact case, the energy flows mainly within the brain, while in the frontal impact case it flows to the neck, where the highest STI is found. Thus, it is possible that the neck acts as an energy flowing path and may sustain injury prior to the brain in a frontal impact. Side impacts with similar loading severity yield much higher
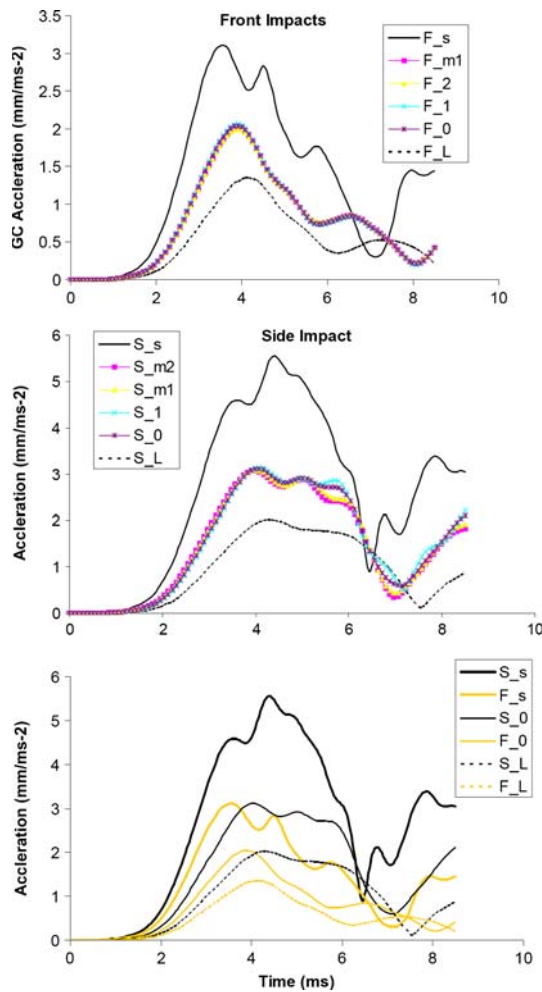
Fig. 10 Gravity centre accelerations and frontal and side impact comparison

Fig. 11 Maximum gravity centre accelerations, HIC and percentage difference with respect to values from frontal impact on original head model

STI than frontal impacts do. A smaller head sustains significantly higher STI both in the frontal and side impacts as seen in Fig. 12, where the length of the vectors are scaled similarly for an easier visual comparison. A similar tendency is also observed for the skull. The skull sustains a much higher STI in a side impact, thus there is a higher probability of fracture for a side impact than for a frontal impact with a similar load severity. Again, a smaller head size yields a much higher STI.

According to the distribution patterns of the STI, in a frontal impact, it is possible that the brain may not be injured, since the neck acts as an outlet of the energy: this conforms to the findings by Zong et al. [9]. For the side impact case, the brain may probably sustain a diffusive injury at the area immediately contiguous to the loading locations. For the skull, the fracture may start from the loading locations for both frontal and side impacts. The fracture in the frontal impact may be a multiple-fracture (linear + compression fracture), which is in agreement
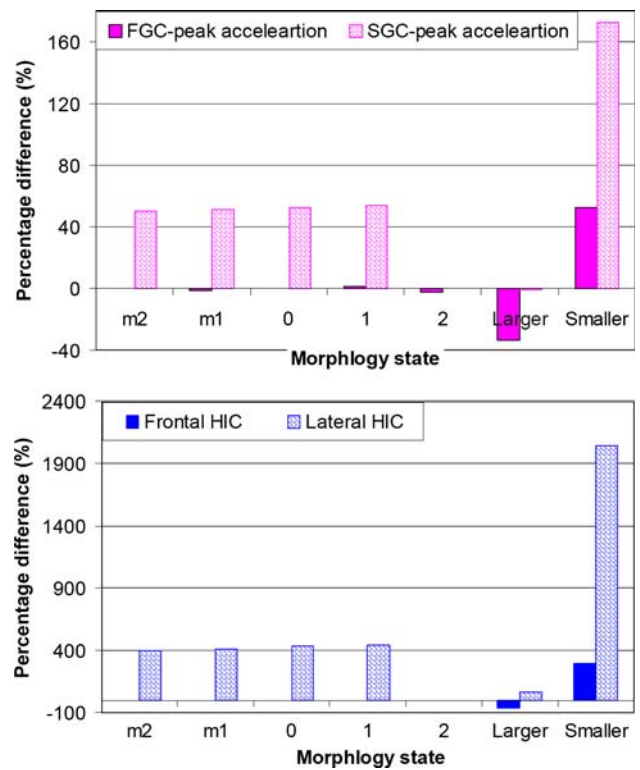
with the experimental observation of Yoganadan et al. [5]. The skull fracture pattern may be circular and diffusive for the side impact case [8].

In summary, there is evidence to suggest that the dynamic response quantities, i.e., the stain energy density, the stress and the maximum tensile strain are quite consistent among themselves and with the STI for the different impact cases. The energy absorptions, the kinematical response quantities of peak gravity centre acceleration and the HIC may not reflect the differences that the different morphological states and the loading locations make. The STI may be a very good representative for all the dynamic skull and brain response quantities to reflect the diffusive injury in place of coup and counter-coup pressure and the local injury for strain, strain and strain energy density.

5 Conclusions

The current finite element simulations have shown that the energy absorption, gravity centre acceleration and HIC may not be the proper criteria for the assessment of head traumatic injury. It is very important to understand how energy is distributed. The STI, which is the vector representation of the energy flow rate, and is consistent with the

Table 8 Peak gravity centre acceleration and HIC

Morphology state	Accleration (mm/ms^{-2})				HIC			
	Frontal impact		Side impact		Frontal impact		Side impact	
	Absolute value	Difference (%)**	Absolute values	Difference (%)**	Absolute values	Difference (%)**	Absolute value	Difference (%)**
m2	NA*	NA*	3.068	50.31	NA*	NA*	4,042.33	398.96
m1	2.018	−1.152	3.090	51.41	798.15	−1.480	4,179.01	415.83
0	2.041	0.000	3.112	52.45	810.15	0.000	4,369.01	439.29
1	2.063	1.051	3.139	53.76	818.70	1.056	4,457.62	450.22
2	1.995	−2.288	NA*	NA*	788.95	−2.616	NA*	NA*
15% larger	1.355	−33.64	2.022	−0.942	304.10	−62.463	1,311.70	61.91
15% smaller	3.106	52.14	5.553	172.05	3,236.36	299.48	17,526.46	2,063.37
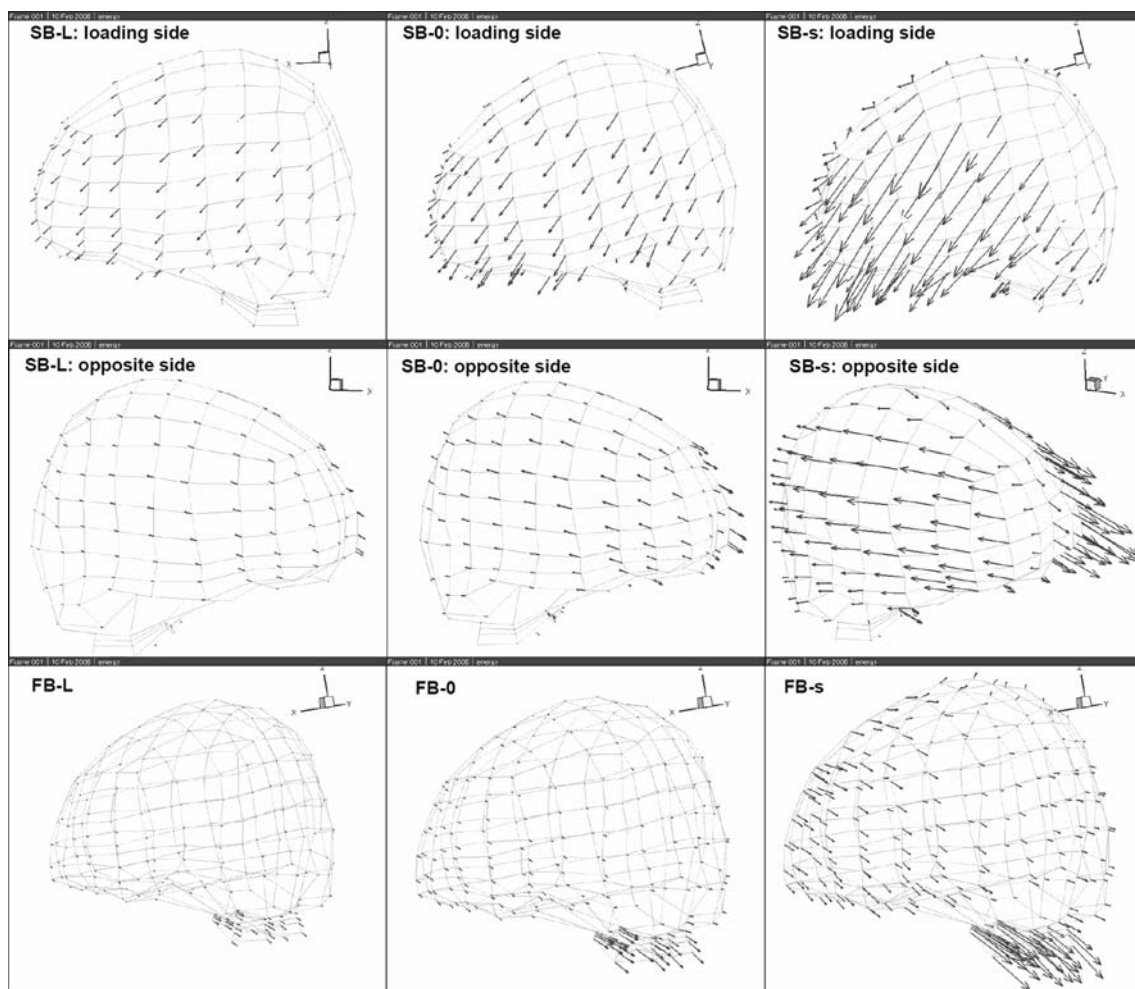
Fig. 12 Maximum STI distributions of brain

dynamic response quantities, could be appropriate for prediction of head traumatic injury. In addition, the STI indicates the location and patterns of skull fracture and brain injury.

A different head morphology has a marginal effect on the head dynamic response quantities and thus the traumatic injury, different locations of the impact loading and head sizes have remarkable effects.
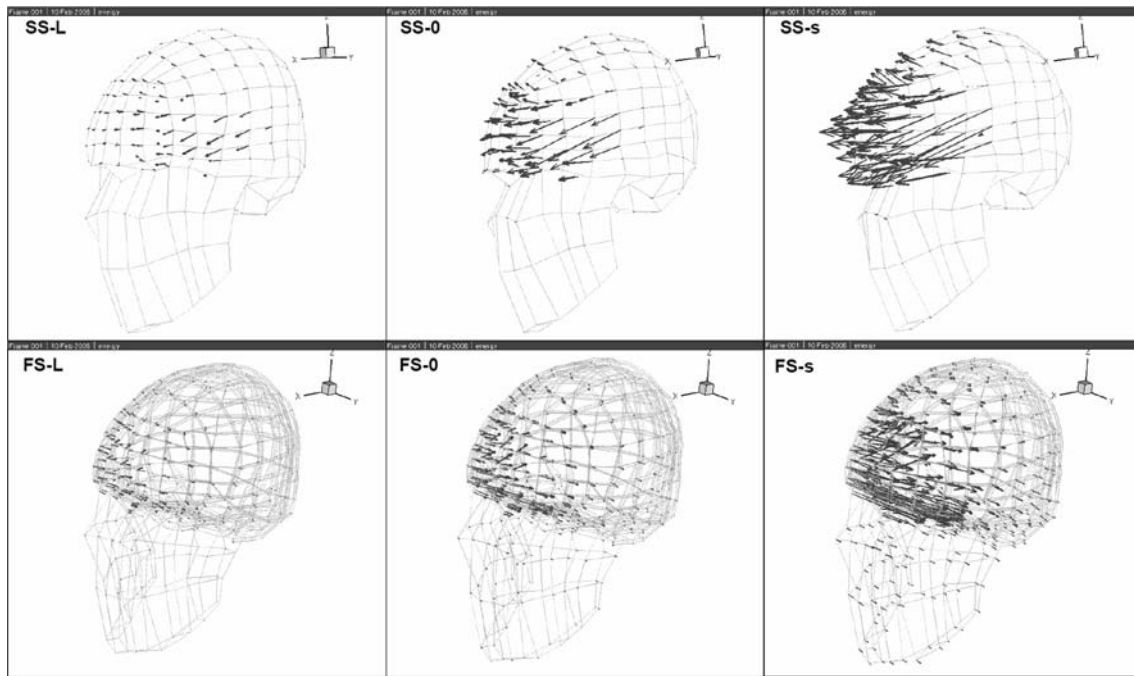
Fig. 13 Maximum STI distributions of skull

References

1. Nahum AM, Smith R (1976) An experimental model for closed head impact injury. In: 20th Stapp Car Crash Conference Proceedings, SAE 760825, Society of Automotive Engineer, Warrendal, Pennsylvania, USA
2. Ruan JS, Khalil TB, King AI (1994) Dynamic response of the human head to impact by three-dimensional finite element analysis. J Biomed Eng 116:44–50
3. O'Donoghue D, Gilchrist MD (1998) Strategies for modeling brain impact injuries. Ir J Med Sci 167(4):263–264
4. Willinger R, Kang HS, Diaw B (2002) Three-dimensional human head finite–element model validation against two experimental impacts. Ann Biomed Eng 27:403–410
5. Yoganadan N, Pintar FA, Sances JrA, Walsh PR, Ewing CL, Thomas DJ, Snyder RG (1995) Biomechanics of skull fractures. J Neurotrauma 12:659–668
6. Zhang LY, Yang KH, King AI (2004) A proposed injury threshold for mild traumatic brain injury. J Biomech Eng-Trans ASME 126:226–236
7. Doorly MC, Phillips JP, Gilchrist MD (2005) Reconstructing real life accidents towards establishing criteria for traumatic head impact injury. In: Proceeding of the UTAM symposium on impact biomechanics: from fundamental insights to applications. University College Dublin, Ireland, pp 81–90
8. Vander VM, Chan P, Zhang J, Yoganadan N, Pintar FA (2004) A new biomechanically-based criterion for side skull fracture. Annu Proc Assoc Ady Automot Med 48:181–195
9. Zong Z, Lee HP, Lu C (2006) A three-dimensional human head finite element model and power flow in a human head subject to impact loading. J Biomech 39(2):284–292
10. Hosey R, Liu YK (1982) A homeomorphic finite element model of the human head and neck. In: Gallagher RH, Simon BR, Johnson PC, Gross JF (eds) Finite element methods in biomechanics, Chapter 18. Wiley, New York, p 379
11. Gilchrist MD, O'Donoghue D, Horgan T (2001) A two dimensional analysis of the biomechanics of frontal and occipital head impact injuries. Int J Crashworthiness 6(2):253–262
12. Horgan TJ, Gilchrist MD (2003) The creation of three-dimensional finite element models for simulating head impact biomechanics. Int J Crashworthiness 8(4):353–366
13. Horgan TJ, Gilchrist MD (2004) Influence of FE model variability in predicting brain motion and intracranial pressure changes in head impact simulations. Int J Crashworthiness 9(4):401–418
14. Viano D, King A, Melvin J, Weber K (1989) Injury biomechanics research: an essential element in the prevention of trauma. J Biomech 22(5):403–417
15. Trosseille X, Lavaste F, Guillon F, Domont A (2002) Development of a FEM of the human head according to a specific test protocol. In: Proceedings of the 36th stapp car crash conf, SAE 922527, Society of Automotive Engineer, Warrendal, Pennsylvania, USA
16. Koenig HA (1998) Modern computational methods. Taylor & Francis, Philadelphia
17. Gilchrist MD, O'Donoghue D (2000) Simulation of the development of frontal head impact injury. Comput Mech 26:229–235
18. Noiseux DU (1970) Measurement of power flow in uniform beams and plates. J Acoust Soc Am 47:238–247
19. Moran B, Shih CF (1987) Crack tip and associated domain integrals from momentum and energy balance. Eng Fracture Mech 27(6):615–641